

DESY 95-104
May 1995

Gluino-Pair Production at the Tevatron

W. Beenakker^{1,2}, R. Höpker¹, M. Spira³ and P. M. Zerwas¹

¹ Deutsches Elektronen-Synchrotron DESY, D-22603 Hamburg, Germany

² Instituut-Lorentz, University of Leiden, The Netherlands [‡]

³ II. Institut f. Theor. Physik [§], Universität Hamburg, D-22761 Hamburg, Germany

ABSTRACT

The next-to-leading order QCD corrections to the production of gluino pairs at the Tevatron are presented in this paper. Similar to the production of squark-antisquark pairs, the dependence of the cross section on the renormalization/factorization scale is reduced considerably by including the higher-order corrections. The cross section increases with respect to the lowest-order calculation which, in previous experimental analyses, had been evaluated at the scale of the invariant energy of the partonic subprocesses.

[‡]present address

[§]Supported by Bundesministerium für Bildung und Forschung (BMBF), Bonn, Germany, under Contract 05 6 HH 93P (5) and by EU Program *Human Capital and Mobility* through Network *Physics at High Energy Colliders* under Contract CHRX-CT93-0357 (DG12 COMA).

1 Physical Set-Up

The novel colored particles in supersymmetric theories, squarks and gluinos, can be searched for most efficiently at high-energy hadron colliders, i. e. the Tevatron $p\bar{p}$ collider and the LHC pp collider in the future. The most stringent lower bounds on squark and gluino masses have been set by the Tevatron experiments CDF and D0. At the 90% CL, the lower limit of the gluino mass was found to be 157 GeV, independent of the squark mass [1, 2].

The cross sections for the production of squarks and gluinos in hadron collisions were predicted at the Born level already quite some time ago [3–6]. Only recently the predictions have been improved by the next-to-leading order QCD contributions for squark-antisquark pair production [7]. In a first step, the *gluon* radiative corrections to gluino pair production have been calculated in Ref.[8]; these corrections are closely related to the gluon corrections for quark-antiquark production, requiring just the appropriate change of the $SU(3)$ Casimir invariants. In this paper we shall present a complete next-to-leading $\mathcal{O}(\alpha_s)$ analysis for gluino pair production,

$$p\bar{p} \rightarrow \tilde{g}\tilde{g} + X \quad (1)$$

including the virtual effects of gluinos and squarks besides gluons and quarks.

The technical set-up of the calculation is analogous to the squark analysis. For the sake of simplicity all squark states are taken mass degenerate. The only free parameters are therefore the masses of squarks and gluinos, $m_{\tilde{q}}$ and $m_{\tilde{g}}$, respectively. (The top mass is fixed to 176 GeV [9, 10].)

The calculation has been performed in the Feynman gauge and the singularities have been isolated by means of dimensional regularization. The masses are renormalized in the on-shell scheme. The massive particles are decoupled smoothly for momenta smaller than their masses in the *modified \overline{MS}* scheme [11]. The soft and the hard gluon radiation are separated by a small invariant mass cut-off parameter Δ for the gluino-gluon and gluino-light quark final states, regularizing the infrared divergences after the virtual corrections are included. If soft and hard gluon emissions are added up, the Δ dependence disappears from the total cross section for $\Delta \rightarrow 0$. The remaining collinear mass singularities are absorbed in the renormalization of the parton densities carried out in the \overline{MS} scheme [12]. We have adopted the GRV [13] and CTEQ(2pM) [14] parametrizations of the parton densities to compare the NLO predictions with the LO approximations; the MRS(H) [15] parametrizations have been included finally to assess the uncertainties of the predictions associated with different parametrizations of the parton densities.

If the gluinos are lighter than the squarks, on-shell squarks can decay into quarks plus gluinos, $\tilde{q} \rightarrow q\tilde{g}$. We will assume in the present analysis that these events are attributed to squark final states; technically, we subtract off the squark-gluino production cross section $qg \rightarrow \tilde{q}\tilde{g}$ after including the non-zero squark width in the propagator. Analogously, the decay of gluinos to squarks is disregarded in the wedge $m_{\tilde{g}} > m_{\tilde{q}}$. Spurious singularities in higher orders at the decay threshold for gluino decays to stop and top, can be regularized by taking the non-zero widths of the particles into account and by performing the mass renormalization of the gluino at the complex pole of the propagator.

The dominant contributions to the production cross sections of gluino pairs in $p\bar{p}$ collisions

are due to the $gg \rightarrow \tilde{g}\tilde{g}$ and the $q\bar{q} \rightarrow \tilde{g}\tilde{g}$ subprocesses. In contrast to squark-pair production, the gg initial state is dominant if both $m_{\tilde{g}}$ and $m_{\tilde{q}}$ are less than about 200 GeV. The qg initial states give rise to $\tilde{g}\tilde{g}$ pairs only at next-to-leading order while the contribution of quark-quark pair initial states to gluino pairs are of yet higher order.

1.1 Gluon-gluon initial states

To lowest order the diagrams contributing to the subprocess $gg \rightarrow \tilde{g}\tilde{g}$ are analogous to the diagrams for quark-pair production, Fig. 1a. Typical standard QCD and supersymmetric vertex corrections are displayed in Fig. 1c. Gluon radiation processes, Fig. 1d, are added incoherently.

Evaluating these diagrams analytically we obtain the double differential cross sections $d\hat{\sigma}_{ij}/d\hat{t}d\hat{u}$ at the parton level; i, j are the parton indices g, q, \bar{q} and \hat{t}, \hat{u} the Mandelstam momentum transfer variables. The total cross sections may be expressed in terms of scaling functions f_{ij} ,

$$\hat{\sigma}_{ij} = \frac{\alpha_s^2(Q^2)}{m_{\tilde{g}}^2} \left\{ f_{ij}^{(0)} + 4\pi\alpha_s(Q^2) \left[f_{ij}^{(1)} + \bar{f}_{ij}^{(1)} \log\left(\frac{Q^2}{m_{\tilde{g}}^2}\right) \right] \right\} \quad (2)$$

The functions f_{ij} depend on the invariant parton energy $\sqrt{\hat{s}}$ and the gluino/squark masses. α_s is the QCD coupling constant. For the sake of simplicity, the renormalization and factorization scales are identified, $\mu_R = \mu_F = Q$. For the non-zero scaling functions $f_{ij}^{(0)}$ to lowest order compact expressions can be derived,

$$f_{gg}^{(0)} = \frac{\pi m_{\tilde{g}}^2}{\hat{s}} \left\{ \left[\frac{9}{4} + \frac{9m_{\tilde{g}}^2}{\hat{s}} - \frac{9m_{\tilde{g}}^4}{\hat{s}^2} \right] \log\left(\frac{1+\beta}{1-\beta}\right) - 3\beta - \frac{51\beta m_{\tilde{g}}^2}{4\hat{s}} \right\} \quad (3)$$

where $\beta = (1 - 4m_{\tilde{g}}^2/\hat{s})^{1/2}$ denotes the gluino velocity in the parton c. m. system. The scaling functions $f_{ij}^{(1)}$ and $\bar{f}_{ij}^{(1)}$, which describe the next-to-leading order corrections, are shown in Fig. 2a in terms of the variable $\eta = \hat{s}/4m_{\tilde{g}}^2 - 1$. The functions $f_{ij}^{(1)}$ are split into the 'virtual+soft' part (V+S) and the 'hard' part (H) in which the infrared $\log^k \Delta$ ($k = 1, 2$) singularities of the (V+S) contribution are absorbed so that the limit $\Delta \rightarrow 0$ can be carried out smoothly. The Sommerfeld rescattering contribution, due to the exchange of Coulomb gluons between the slowly moving gluinos in the final state, leads to a singularity $\sim \pi\alpha_s/\beta$ near the threshold, which compensates the phase space suppression. In addition, soft gluons give rise to a logarithmic enhancement near threshold,

$$f_{gg}^{(1)thr} = f_{gg}^{(0)thr} \left\{ \frac{1}{16\beta} + \frac{3}{2\pi^2} \log^2(8\beta^2) - \frac{29}{4\pi^2} \log(8\beta^2) \right\} \quad (4)$$

with

$$f_{gg}^{(0)thr} = \frac{27\pi\beta}{64}$$

For large parton energies, the \hat{t} - and \hat{u} -channel exchanges of gluons generate an asymptotically constant cross section $\hat{\sigma} \sim \alpha_s^3/m_{\tilde{g}}^2$. This is to be contrasted with the scaling behavior $\hat{\sigma}_{LO} \sim \alpha_s^2/\hat{s}$ in lowest order. The asymptotic values of the corresponding scaling functions are given by $f_{gg}^{(1)} \rightarrow 1949/(800\pi)$ and $\bar{f}_{gg}^{(1)} \rightarrow -177/(160\pi)$.

1.2 Quark-antiquark initial states

In addition to the annihilation via \hat{s} -channel gluon exchange, also \hat{t} - and \hat{u} -channel squark exchanges contribute to the process $q\bar{q} \rightarrow \tilde{g}\tilde{g}$, Fig. 1b. To lowest order the cross section is given by the function

$$f_{q\bar{q}}^{(0)} = \frac{\pi m_{\tilde{g}}^2}{\hat{s}} \left\{ \beta \left[\frac{20}{27} + \frac{16m_{\tilde{g}}^2}{9\hat{s}} - \frac{8m_-^2}{3\hat{s}} + \frac{32m_-^4}{27(m_-^4 + m_{\tilde{g}}^2\hat{s})} \right] + \left[\frac{64m_{\tilde{g}}^2}{27\hat{s}} + \frac{8m_-^4}{3\hat{s}^2} - \frac{16m_{\tilde{g}}^2m_-^2}{27\hat{s}(\hat{s} - 2m_-^2)} \right] \log \left(\frac{1 - \beta - 2m_-^2/\hat{s}}{1 + \beta - 2m_-^2/\hat{s}} \right) \right\} \quad (5)$$

where we have introduced the abbreviation $m_-^2 = m_{\tilde{g}}^2 - m_{\tilde{q}}^2$. The LO cross section is small for equal gluino and squark masses due to the negative interference between the three diagrams. This is also the case in next-to-leading order. The scaling functions $f_{q\bar{q}}^{(1)}$ and $\bar{f}_{q\bar{q}}^{(1)}$ associated with the next-to-leading order corrections are displayed in Fig. 2b. At the threshold, the cross section is non-zero due to the Sommerfeld enhancement,

$$f_{q\bar{q}}^{(1)thr} = f_{q\bar{q}}^{(0)thr} \left\{ \frac{3}{16\beta} + \frac{2}{3\pi^2} \log^2(8\beta^2) - \frac{41}{12\pi^2} \log(8\beta^2) \right\} \quad (6)$$

with

$$f_{q\bar{q}}^{(0)thr} = \frac{\pi\beta}{3} \left(\frac{m_{\tilde{g}}^2 - m_{\tilde{q}}^2}{m_{\tilde{g}}^2 + m_{\tilde{q}}^2} \right)^2$$

Since any \hat{t} - or \hat{u} -channel gluon exchange diagrams are absent, the scaling functions vanish for asymptotic energies.

1.3 Quark-gluon initial states

Gluino pairs can be produced in quark-gluon collisions only in higher orders, $f_{qg}^{(0)} = 0$, [cf. Fig. 1d with the bottom gluon line replaced by a quark line]. The corresponding scaling functions $f_{qg}^{(1)}$ and $\bar{f}_{qg}^{(1)}$ are small, in the Tevatron range, compared with the $q\bar{q}, gg$ scaling functions as shown in Fig. 2c. The gluon exchange in the \hat{t} - and \hat{u} -channel gives rise asymptotically to a non-vanishing cross section of order $\alpha_s^3/m_{\tilde{g}}^2$ with $f_{qg}^{(1)} \rightarrow 1949/(3600\pi)$ and $\bar{f}_{qg}^{(1)} \rightarrow -59/(240\pi)$.

2 Results

The final results for the cross section $p\bar{p} \rightarrow \tilde{g}\tilde{g}X$ are presented in Fig. 3 and Fig. 4. The cross sections of the subprocesses have been convoluted with the parton densities in the GRV [13], CTEQ(2pM) [14] and MRS(H) [15] parametrizations. The detailed analysis of these figures leads us to the following conclusions.

(i) It is obvious from Fig. 3a that the theoretical predictions for the $p\bar{p} \rightarrow \tilde{g}\tilde{g}$ production process are greatly stabilized by taking into account the next-to-leading order QCD corrections. While the dependence on the renormalization/factorization scale Q is quite steep

and monotonic in leading order, the Q dependence is significantly reduced in next-to-leading order for reasonable variations of the scale. Close to $Q \sim m_{\tilde{g}}/2$ even a broad maximum develops. The variation of the cross section for different NLO parton parametrizations is very small.

(ii) In contrast to squark-pair production, the K -factors for gluino pair production, $K = \sigma_{NLO}/\sigma_{LO}$ (with all quantities in the numerator and denominator calculated consistently in NLO and LO, respectively), depend rather strongly on the gluino and squark masses, Fig. 3b, in particular in the range where squark and gluino masses nearly coincide.

(iii) In Fig. 4 we illustrate the impact of the QCD corrections on the experimental bound on the gluino mass. The scale $\sqrt{\hat{s}}$ had been adopted in the experimental analyses, which were based on LO cross sections. We therefore compare the LO cross section, defined at this scale, with the NLO prediction evaluated at the scale $Q = m_{\tilde{g}}$. As evident from the figure, this increases the bound on the gluino mass by a shift between 10 and 30 GeV, depending in detail on $m_{\tilde{g}}$ itself and on $m_{\tilde{q}}$. By comparing the NLO prediction with the LO result in Fig. 4, it is clear that the bounds extracted by the Tevatron experiments are conservative and that the true bounds are likely to be higher at a level of 10 to 30 GeV.

Acknowledgment. We thank S. Lammel for useful discussions on the Tevatron squark and gluino mass limits.

References

- [1] CDF Collaboration, F. Abe *et al.*, Phys. Rev. Lett. **69** (1992) 3439.
- [2] S. Hagopian, Proceedings of the XXVII Int. Conf. on High Energy Physics, Glasgow (1994) and FERMILAB Conf 94/ 331-E (1994); D. R. Claes, FERMILAB Conf 94/ 290-E (1994); S. Lammel, talk at the DESY Theory Workshop on Supersymmetry, Hamburg (1994).
- [3] G. L. Kane and J. P. Leveille, Phys. Lett. **B 112** (1982) 227.
- [4] P. R. Harrison and C. H. Llewellyn Smith, Nucl. Phys. **B213** (1983) 223; (E) **B223** (1983) 542.
- [5] E. Reya and D. P. Roy, Phys. Rev. **D 32** (1985) 645.
- [6] H. Baer, F. E. Paige, S. D. Protopopescu and X. Tata, Report on ISAJET 7.0/ ISASUSY 1.0, FSU-HEP 930329 and UH-511-764-93.
- [7] W. Beenakker, R. Höpker, M. Spira and P.M. Zerwas, Phys. Rev. Lett. **74** (1995) 2905.
- [8] W. Beenakker, H. Kuijf, W. L. van Neerven and J. Smith, Phys. Rev. **D 40** (1989) 54.
- [9] CDF Collaboration, F. Abe *et al.*, Phys. Rev. Lett. **73** (1994) 225; Phys. Rev. **D 50** (1994) 2966; Phys. Rev. Lett. **74** (1995) 2626.
- [10] D0 Collaboration, S. Abachi *et al.*, Phys. Rev. Lett. **74** (1995) 2632.
- [11] J. Collins, F. Wilczek and A. Zee, Phys. Rev. **D 18** (1978) 242; W. J. Marciano, Phys. Rev. **D 29** (1984) 580; P. Nason, S. Dawson and R. K. Ellis, Nucl. Phys. **B303** (1988) 607.
- [12] G. Altarelli, R. K. Ellis and G. Martinelli, Nucl. Phys. **B157** (1979) 461; W. Furmanski and R. Petronzio, Z. Phys. **C 11** (1982) 293.
- [13] M. Glück, E. Reya and A. Vogt, Z. Phys. **C 53** (1992) 127.
- [14] J. Botts, J.G. Morfin, J.F. Owens, J. Qiu, W.-K. Tung and H. Weerts, CTEQ Collaboration, Phys. Lett. **B 304** (1993) 159; J. Botts, H.L. Lai, J.G. Morfin, J.F. Owens, J. Qiu and W.-K. Tung, CTEQ2 Collaboration, MSUHEP-93/28 (1993).
- [15] A.D. Martin, W.J. Stirling and R.G. Roberts, Proceedings, Workshop on Quantum Field Theoretical Aspects of High Energy Physics, B. Geyer and E.-M. Ilgenfritz (eds.), ZHS Univ. Leipzig (1993).

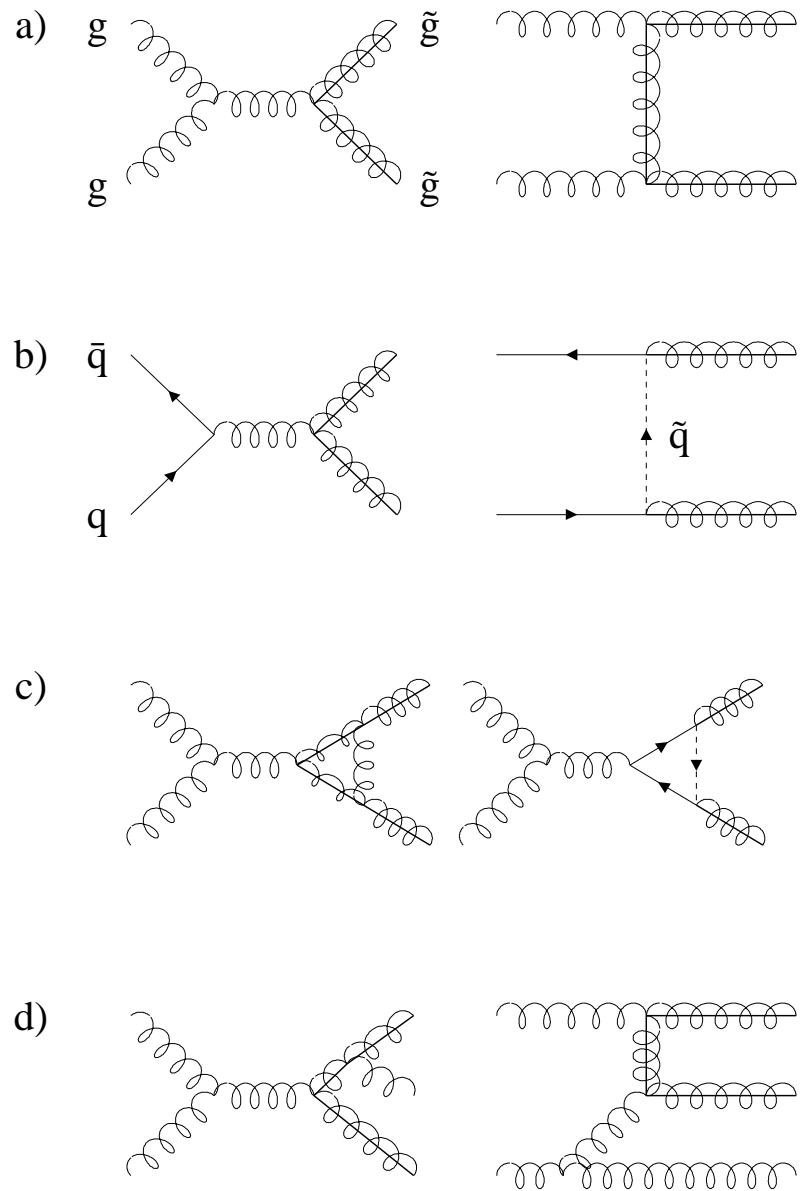


Figure 1: Generic diagrams for gluino-pair production: a) Born-level gg diagrams; b) Born-level $q\bar{q}$ diagrams; c) QCD and SUSY vertex corrections; d) Bremsstrahlung diagrams, and qg parton processes if the bottom gluon line is replaced by a quark line.

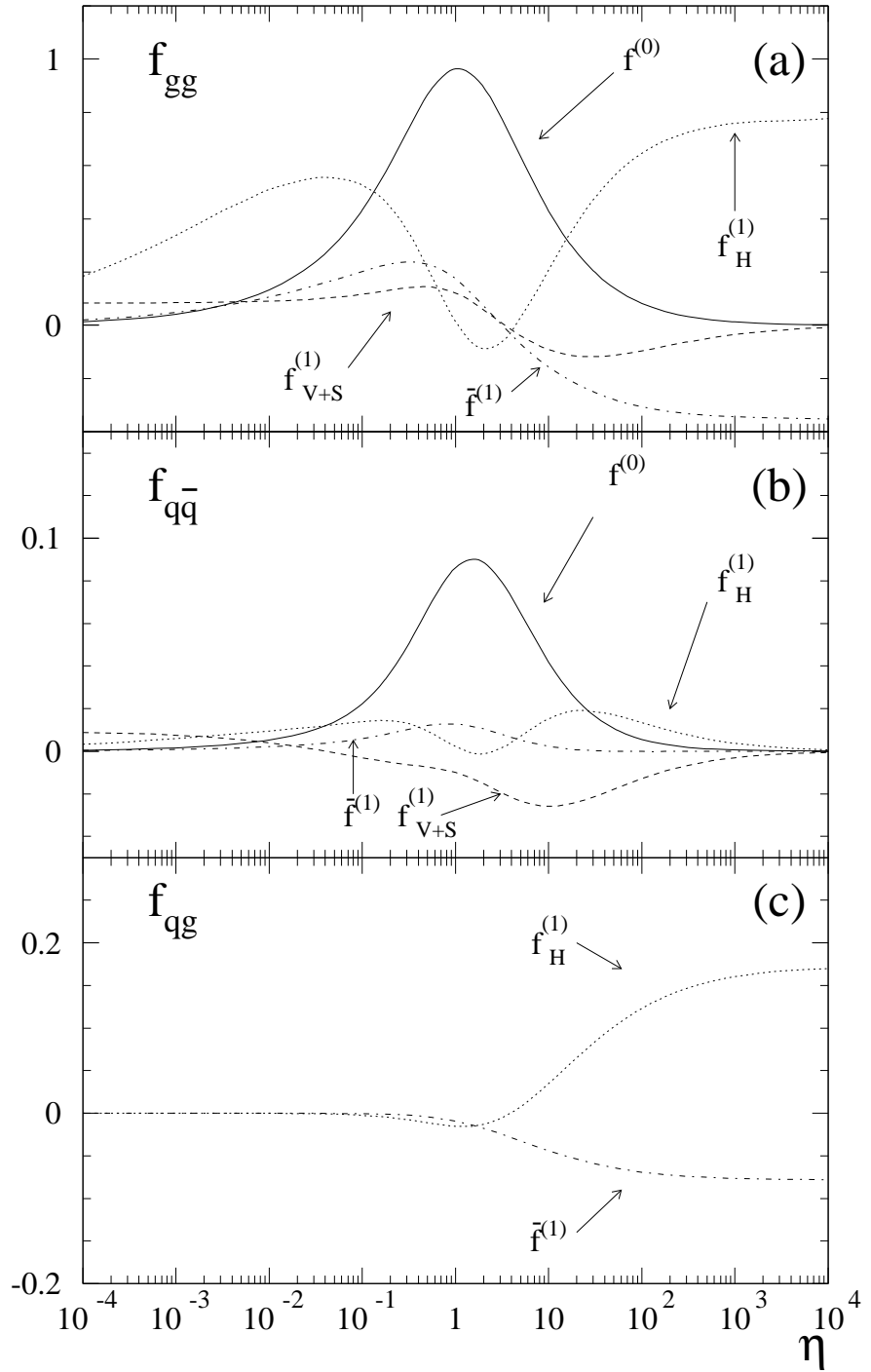


Figure 2: The scaling functions for gluino-pair production in a) gg , b) $q\bar{q}$ and c) qg collisions. The notation follows eq. (2) with $\eta = \hat{s}/4m_{\tilde{g}}^2 - 1$; mass parameters: $m_{\tilde{g}} = 250$ GeV and $m_{\tilde{q}} = 200$ GeV.

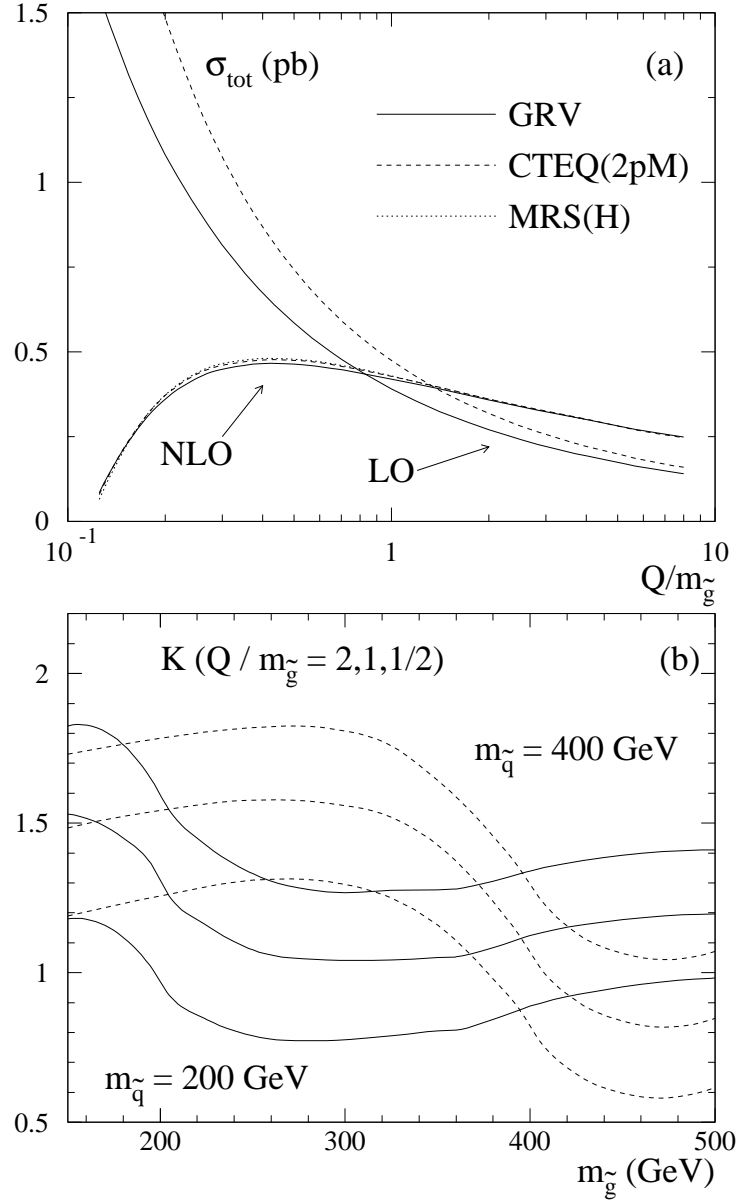


Figure 3: Total cross section for gluino-pair production at the Tevatron energy $\sqrt{s} = 1.8$ TeV. a) Dependence on the scale Q for the LO and NLO predictions, and sensitivity to different parton densities; mass parameters: $m_{\tilde{g}} = 250$ GeV and $m_{\tilde{q}} = 200$ GeV. b) K factors for the scales $Q/m_{\tilde{g}} = 2, 1, 1/2$, corresponding to upper, middle and lower curves, respectively; GRV parton densities.

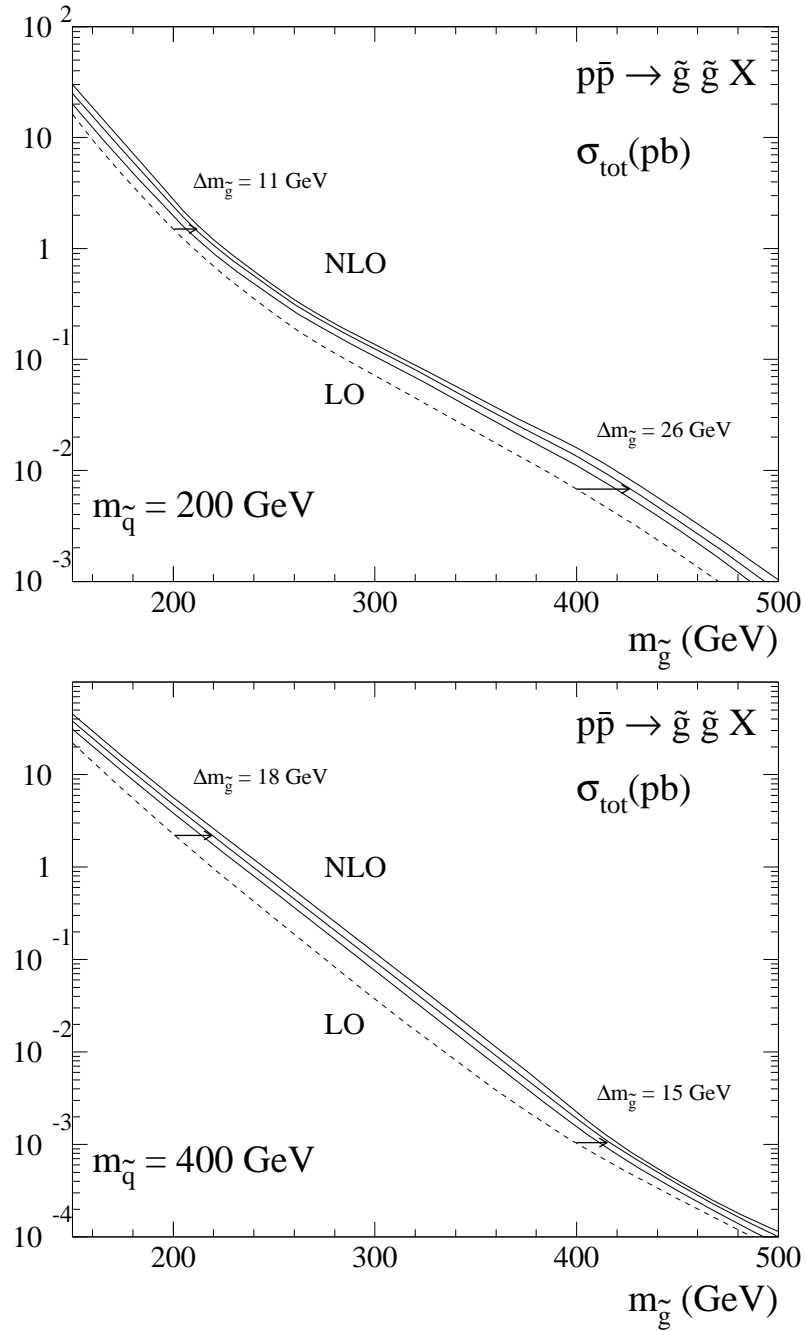


Figure 4: Total cross section for gluino-pair production at the Tevatron energy $\sqrt{s} = 1.8$ TeV. Dependence of the cross section on the gluino mass; LO with EHLQ parton densities and $Q = \sqrt{s}$ and NLO with GRV parton densities at the scales $Q/m_{\tilde{g}} = 2, 1, 1/2$ corresponding to lower, middle and upper curve, respectively.